23rd ABCM International Congress of Mechanical Engineering
December 6-11, 2015, Rio de Janeiro, RJ, Brazil

Linear Instability in RBP Convection for Viscoelastic Fluids

S. C. Hirata
M. N. Ouarzazi
Laboratoire de Mécanique de Lille, UMR CNRS 8107, Université Lille 1, Bld. Paul Langevin, 59655 Villeneuve d′Ascq cedex, France
silvia.hirata@univ-lille1.fr, najib.ouarzazi@univ-lille1.fr

L. S. de B. Alves
Laboratório de Mecânica Teórica e Aplicada, Departamento de Engenharia Mecânica, Universidade Federal Fluminense, Rua Passo da Pátria 156, Niterói, RJ 24210-240, Brazil
leonardo.alves@gmail.com

Abstract. *A linear stability analysis is performed in order to determine the onset of convective and absolute instabilities in Rayleigh-Bénard-Poiseuille mixed convection for viscoelastic fluids. The viscoelastic fluid is modeled by means of a general constitutive equation that encompasses the Maxwell model and the Oldroyd-B model. In comparison to Newtonian fluids, two more dimensionless parameters are introduced, namely the retardation and the relaxation times. Temporal stability analysis of the basic state showed that the three-dimensional thermoconvective problem can be Squire-transformed. In the limit of zero throughflow ($Re = 0$), two different regimes can be distinguished : the weakly elastic regime, where the emerging structures are stationary; and the strongly elastic regime, where the convective structures are oscillatory. The thresholds for the appearance of longitudinal rolls (LRs) are independent of Re. For transverse rolls (TRs), it is found that in the weakly elastic regime, the stabilization effect of Re is more important than in Newtonian fluids. In the strongly elastic regime, the effect of the imposed throughflow is to promote the appearance of the up-stream moving TRs for low values of Re which are replaced by the down-stream moving TRs for higher values of Re. The influence of the rheological parameters on the transition curves from convective to absolute instability in the Reynolds-Rayleigh plane is also determined by means of a spatiotemporal analysis. We show that the viscoelastic character of the fluid hastens the transition to absolute instability and even may suppress the convective/absolute transition. Throughout this paper, similarities and differences with the corresponding problem for Newtonian fluids are highlighted.*

Keywords: *thermoconvective instabilities, viscoelastic fluids, linear stability analysis*

1. INTRODUCTION

The classical Rayleigh-Bénard-Poiseuille (RBP) problem consists of a fully-developed mixed-convection problem, which results from the superposition of a horizontal pressure gradient and a vertical temperature gradient. In most cases, RBP systems are uniformly heated from below and submitted to a unidirectional throughflow with a laminar parabolic velocity profile due to the low Reynolds number imposed. In the conductive state, i.e. when the Rayleigh number is smaller than its first critical value, a Poiseuille flow is observed. When buoyancy forces are strong enough to overcome viscous forces, different types of thermoconvective structures can appear. We do not review here the numerous studies devoted to RBP flows of Newtonian fluids, but instead refer to the exhaustive bibliographical review presented by Nicolas (2002) .

In open systems (such as the RBP system), both the temporal and spatial growth of the disturbances must be considered and one must distinguish between the convective and the absolute nature of the instability. A methodology for doing so was applied towards two-dimensional hydrodynamic instabilities by Huerre and Monkewitz (1985, 1990). It consists of analyzing the evolution and asymptotic behavior of wave packets initially subjected to an impulse excitation. If its amplitude decays as it is advected downstream by the base flow, the system is convectively stable. Otherwise, the system is unstable. Two possibilities arise in the latter case. If the amplitude of an initially localized disturbance enveloppe eventually decays at any fixed location while it grows when observed in a coordinate system moving with its group speed, the system is convectively unstable. Otherwise, the system is absolutely unstable. Hence, all disturbances eventually leave a convectively unstable system in the absence of external forcing capable of providing a continuous perturbation source, allowing the system to return to its base state. On the other hand, certain disturbances initially present in an absolutely unstable system will eventually grow in time, forcing this system away from its original base state. In such cases, low amplitude forcing plays a marginal role because the system becomes self-excited.

Even though buoyancy-driven instabilities in Newtonian fluids have been extensively studied, the same cannot be said about their non-Newtonian counterparts. This is probably due to the fact that there is often a highly non trivial coupling between the thermal-hydrodynamic problem and the rheological constitutive equation of the fluid. Recently, the scientific community has been showing an increasing interest in mixed convection of non-Newtonian fluids. The reason for this is that such fluids can be found in a great number of applications, such as those in the food, cosmetics, pharmaceutical and petroleum industries, among others. More specifically, mixed convection of viscoelastic fluids through pipes and channels are relevant in polymer processing, where the melt flows at high temperatures before the extrusion process. In order to avoid the appearance of non-homogeneities in the final product, it is necessary to control the instabilities in the melt flow. Therefore, knowledge of the convective behavior of the flow is an essential requirement to the design of polymer processing equipment.

For viscoelastic fluids, linear stability analysis reveals that the onset of Rayleigh-Benard (natural) convection can be oscillatory instead of stationary, depending on the fluid elasticity. This behavior was confirmed by the experimental results of Kolodner (1998) using DNA suspensions. Such a viscoelastic instability is usually observed in dilute polymer solutions, consisting of a Newtonian solvent and a polymeric solute. These solutions can be highly elastic while maintaining an essentially constant viscosity. They are, therefore, well represented by the Oldroyd-B constitutive model (Bird et al., 1987). As argued by Li and Khayat (2005), two regimes can be distinguished in the RB convection of an Oldroyd-B fluid: the weakly and strongly elastic regimes. In the absence of throughflow, weakly (strongly) elastic fluids are identified as fluids with elasticity number smaller (larger) than λ_1^f, where λ_1^f is the critical elasticity number for the onset of oscillatory convection.

To the best of our knowledge, the RBP convection of a viscoelastic fluid has not been considered before in the literature. Therefore, the major goal of the current work is to investigate the influence of elasticity effects on the physical mechanisms driving linear spatio-temporal instabilities in this flow of great technological importance. Our focus lies on a three-dimensional temporal linear stability analysis to determine the onset of convective instability. A two-dimensional spatial linear stability analysis is also utilized to distinguish it from the onset of absolute instability for TRs.

2. PROBLEM FORMULATION

2.1 Governing equations

Consider an incompressible Oldroyd-B fluid layer of depth h in the vertical z-direction, with $z^* = 0$ at its center. This layer has an infinite extent in the x and y directions. Upper and lower horizontal walls are kept at constant temperatures T_0^* and T_1^* ($> T_0^*$), respectively, and a constant pressure gradient is imposed in the x-direction. All physical properties are assumed constant and evaluated at T_0^*. They are given by ν for kinematic viscosity, μ for dynamic viscosity, K for thermal diffusivity, ρ for density, β for thermal expansion coefficient, g for gravitational acceleration and, finally, λ_1^* and λ_2^* for relaxation and retardation times of the viscoelastic fluid, respectively. Assuming the Oberbeck-Boussinesq approximation holds, the governing equations for this problem are

$$\nabla . \mathbf{u}^* = 0 \tag{1}$$

$$\rho \left(\frac{\partial \mathbf{u}^*}{\partial t^*} + (\mathbf{u}^* . \nabla)\, \mathbf{u}^* \right) = -\, \nabla P^* + \nabla . \tau^* + \rho\, \beta\, (T^* - T_0^*)\, \underline{g}\, \mathbf{e_z} \tag{2}$$

$$\frac{\partial T^*}{\partial t^*} + (\mathbf{u}^* . \nabla)\, T^* = K\, \nabla^2 T^* \tag{3}$$

$$\tau^* + \lambda_1^*\, (\tau^*)^{\nabla} = \mu \left(\gamma^* + \lambda_2^*\, (\gamma^*)^{\nabla} \right) \tag{4}$$

The upper convected, or Oldroyd, time derivative is defined as:

$$(\tau^*)^{\nabla} = \frac{\partial \tau^*}{\partial t^*} + (\mathbf{u}^* . \nabla) \tau^* - (\nabla \mathbf{u}^*)^T . \tau^* - \tau^* . (\nabla \mathbf{u}^*) \tag{5}$$

where $\mathbf{u}^*$, P^* and T^* represent the velocity, hydrostatic pressure, and temperature fields, respectively, τ^* is the stress tensor and γ^* is the strain rate tensor. The above equations are subject to the following horizontal wall boundary conditions,

$$\mathbf{u}^* = 0 \quad \text{at} \quad z^* = \pm \frac{h}{2} \tag{6}$$

$$T^* = T_0^* \quad \text{at} \quad z^* = + \frac{h}{2} \quad \text{and} \quad T^* = T_1^* \quad \text{at} \quad z^* = - \frac{h}{2} \tag{7}$$

2.2 Base state and linear stability analysis

System of equations (1) to (5), subjected to boundary conditions (6) and (7), has a steady-state that corresponds to a combination of the plane Poiseuille flow with vertical thermal stratification. This base flow is written as

$$\mathbf{u}_b^* = U_0^* \left(1 - 4\, \frac{z^{*2}}{h^2} \right) \mathbf{e_x}, \tag{8}$$

$$T_b^* = T_0^* + (T_1^* - T_0^*)\left(\frac{1}{2} - \frac{z^*}{h}\right), \tag{9}$$

$$P_b^* = P_0^* + \frac{\rho\,\beta\,g\,h\,(T_1^* - T_0^*)}{2}\left(\frac{z^*}{h} - \frac{z^{*2}}{h^2}\right) - \frac{8\,\mu\,U_0^*}{h}\left(\frac{x^*}{h}\right), \tag{10}$$

with U_0^* being defined as the maximum steady-state throughflow velocity. This solution has an associated stress tensor with three non-zero components.

The shear stress components $(\tau_b^*)^{(1,3)} = (\tau_b^*)^{(3,1)} = -8\,(U_0^*\,\mu/h^2)\,z^*$ also appear for Newtonian fluids and vary linearly across the vertical channel section. For the Oldroyd-B model, this linear variation in the vertical direction of the shear stress components induces quadratic variations in normal stress component $(\tau_b^*)^{(1,1)} = 128\,\mu\,(\lambda_1^* - \lambda_2^*)\,(U_0^{*2}/h^4)\,(z^*)^2$. This component vanishes for Newtonian fluids (i.e. $\lambda_1^* = \lambda_2^*$) .

Once the base flow has been defined, one can verify its asymptotic ($t \to \infty$) stability by following the classical linear stability formalism. In order to do so, dependent variables in the governing equations (1) to (7) are replaced by this base flow superposed with infinitesimal perturbations. Since these perturbations are considered small, one can linearize the resulting equations to deduce the perturbation governing equations.

The dimensionless parameters appearing in the governing equations are the Rayleigh number Ra, Reynolds number Re, Prandtl number Pr, dimensionless relaxation time or elasticity number λ_1 and dimensionless retardation time λ_2. These numbers are respectively defined as : $Ra = \frac{g\,\beta\,\Delta T^*\,h^3}{\nu\,K}$, $Re = \frac{U_0^*\,h}{\nu}$, $Pr = \frac{\nu}{K}$, $\lambda_1 = \frac{\lambda_1^*}{h^2/K}$, $\lambda_2 = \frac{\lambda_2^*}{h^2/K}$, where the ratio between retardation and relaxation times $\Gamma = \lambda_2^*/\lambda_1^*$ is used in this study instead of λ_2. Typical fluids satisfying constitutive relation (4) are solutions composed of a Newtonian solvent and a polymeric solute with viscosities μ_s and μ_p, respectively. The viscosity of the solution is given by $\mu = \mu_s + \mu_p$ and, hence, the ratio between retardation and relaxation times is $\Gamma = \mu_s/\mu$ (Bird et al., 1987). Finally, it should be noted that $\lambda_1 <= \lambda_2$, i.e. $\Gamma \in [0,1]$ and that the Maxwellian model is recovered when $\Gamma = 0$ (or $\lambda_2 = 0$) whereas the Newtonian model is recovered when $\Gamma = 1$ (or $\lambda_1 = \lambda_2$).

Following the classical linear stability procedure, we seek three-dimensional normal modes in the form

$$\left\{w_p, \theta_p, \tau_p^{(i,j)}\right\}(x,y,z,t) = \left\{w_n, \theta_n, \tau_n^{(i,j)}\right\}(z)\,\exp\big(i\,(k_x\,x + k_y\,y - \omega\,t)\big) \tag{11}$$

where k_x and k_y are the wave numbers in the x- and y-directions, respectively, and ω is the frequency. All three parameters are complex numbers, since both temporal and spatial stability analyses were performed in the present study. Upon substitution of functional form (11) into the linearized equations, it is possible to reduce the resulting system to two coupled ordinary differential equations for the linear perturbation normal mode amplitudes $w_n(z)$ and $\theta_n(z)$. They are given by

$$\begin{aligned}\frac{i}{Pr}\Big(\big(k_x\,Re\,Pr\,f(z) - \omega\big)\big(\mathrm{D}^2 - k^2\big) - k_x\,Re\,Pr\,f''(z)\Big)\,w_n(z) + k^2\,\mathrm{D}\,\tau_n^{(3,3)}(z)&\\ + \mathrm{D}\,\mathrm{L}\big(w_n(z)\big) + \big(\mathrm{D}^2 + k^2\big)\,\mathrm{J}\big(w_n(z)\big) + Ra\,k^2\,\theta_n(z) = 0\,,&\end{aligned} \tag{12}$$

$$w_n(z) + \big(\mathrm{D}^2 - k^2 - i\,k_x\,Re\,Pr\,f(z) + i\,\omega\big)\,\theta_n(z) = 0 \tag{13}$$

where $k^2 = k_x^2 + k_y^2$, $\mathrm{D} = \mathrm{d}/\mathrm{d}z$ and the dependence of operators L and J, as well as stress component $\tau^{(3,3)}(z)$, on $w_n(z)$ is given by expressions

$$\begin{aligned}\mathrm{L}\big(w_n(z)\big) &= -k_x^2\,\tau_n^{(1,1)}(z) - k_y^2\,\tau_n^{(2,2)}(z) - 2\,k_x\,k_y\,\tau_n^{(1,2)}(z)\\ &= \Big(2\,i\,k_x\,Re\,Pr\,\lambda_1\,f'(z)\,\mathrm{J}\big(w_n(z)\big) + \Big(2\,i\,k_x\,Re\,Pr\,\lambda_1\,(2\,\Gamma - 1)\,f'(z)\,\mathrm{D}^2\\ &+ 4\,k_x^2\,Re^2\,Pr^2\,\lambda_1^2\,(1-\Gamma)\,\big(f'(z)\big)^2 + 2\,k^2 + 2\,i\,k^2\,k_x\,Re\,Pr\,\lambda_1\,\Gamma\,f(z)\\ &- 2\,i\,k^2\,\omega\,\lambda_1\,\Gamma\,\mathrm{D} + 4\,k_x^2\,Re^2\,Pr^2\,\lambda_1^2\,(1-\Gamma)\,f'(z)\,f''(z)\\ &+ 2\,i\,k^2\,k_x\,Re\,Pr\,\lambda_1\,\Gamma\,f'(z)\Big)\,w_n(z)\Big)\Big/\big(1 + i\,k_x\,Re\,Pr\,\lambda_1\,f(z) - i\,\omega\,\lambda_1\big)\,,\end{aligned} \tag{14}$$

$$
\begin{aligned}
\mathrm{J}\big(w_n(z)\big) \;&=\; i\,k_x\,\tau_n^{(1,3)}(z) + i\,k_y\,\tau_n^{(2,3)}(z) \\
&=\; \Big(i\,k_x\,Re\,Pr\,\lambda_1\,f\,'(z)\,\tau_n^{(3,3)}(z) - \Big(2\,i\,k_x\,Re\,Pr\,\lambda_1\,\Gamma\,f\,'(z)\,\mathrm{D} - i\,\omega\,\lambda_1\,\Gamma\,\mathrm{D}^2 \\
&+\; \big(1+k^2\big)\big(1 + i\,k_x\,Re\,Pr\,\lambda_1\,\Gamma\,f(z)\big) + i\,k_x\,Re\,Pr\,\lambda_1\,(1-\Gamma)\,f\,''(z) - i\,\omega\,k^2\,\lambda_1\,\Gamma \\
&+\; 2\,k_x^2\,Re^2\,Pr^2\,\lambda_1^2\,(1-\Gamma)\,\big(f\,'(z)\big)^2\Big)\,w_n(z)\Big)\Big/\big(1 + i\,k_x\,Re\,Pr\,\lambda_1\,f(z) - i\,\omega\,\lambda_1\big)\,,
\end{aligned}
\tag{15}
$$

$$
\begin{aligned}
\tau_n^{(3,3)}(z) \;&=\; \Big(\big((2 + 2\,i\,k_x\,Re\,Pr\,\lambda_1\,\Gamma\,f(z) - 2\,i\,\omega\,\lambda_1\,\Gamma)\,\mathrm{D} \\
&+\; 2\,i\,k_x\,Re\,Pr\,\lambda_1\,(1-\Gamma)\,f\,'(z)\big)\big/\big(1 + i\,k_x\,Re\,Pr\,\lambda_1\,f(z) - i\,\omega\,\lambda_1\big)\Big)\,w_n(z)\,,
\end{aligned}
\tag{16}
$$

For the sake of conciseness, expressions of the other components of the stress tensor have been omitted, and can be found elsewhere (Hirata et al. (2015)). Boundary conditions become

$$w_n = \mathrm{D}\,w_n = 0 \quad \text{at} \quad z = \pm 1/2\,, \tag{17}$$

$$\theta_n = 0 \quad \text{at} \quad z = \pm 1/2. \tag{18}$$

3. REVIEW OF THE LINEAR STABILITY IN THE ABSENCE OF THROUGHFLOW

Before discussing throughflow effects on viscoelastic instabilities, an overview of linear stability results in the absence of throughflow is presented. Li and Khayat (2005) distinguish two different regimes in this limit, i.e. when $Re = 0$. The so-called weakly elastic regime corresponds to the parameter set where the conductive base state first bifurcates to a stationary convective state. Otherwise, in the strongly elastic regime, the onset of convection is oscillatory. Approximate results for both regimes can be generated with an algebraic dispersion relation obtained from a single term Galerkin expansion. It is then possible to estimate the parameter set that locates the boundary separating weakly and strongly elastic regimes. For fixed values of Γ and Pr, there exists a value of $\lambda_1 = \lambda_1^f$ where $Ra_c^s = Ra_c^o$. In other words, both critical Rayleigh numbers for the onsets of stationary and oscillatory convection coincide at well defined parametric conditions and, therefore, a codimension-two bifurcation occurs. This behavior is illustrated in Fig. 1, which shows λ_1^f isolines on a (Γ, λ_1) plane for different values of Pr obtained from the single term Galerkin expansion. Three cases for each solution type plus a Maxwell fluid were analyzed, and they are marked as asterisks in Fig. 1. Each case is correlated with one or two more cases, enabling a qualitative trend analysis. Furthermore, throughout this paper we shall assume $Pr = 10$ unless stated otherwise.

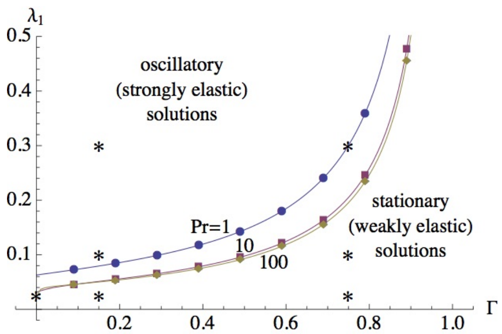

Figure 1. Elasticity levels λ_1^f defining the crossover between stationary (weakly elastic) and oscillatory (strongly elastic) bifurcations, for $Re = 0$ and $Pr = 1$, 10 and 100. Results were obtained with the single term Galerkin expansion. Stars indicate representative pairs of (Γ, λ_1) used in computations throughout the paper.

4. CONVECTIVE INSTABILITY

After this brief discussion of the main thermal instability mechanisms that exist for viscoelastic fluids in the absence of throughflow, its effect can now be properly studied. When doing so, weakly and strongly elastic regimes are analyzed separately through an appropriate selection of elasticity λ_1 and viscosity ratio Γ pairs for $Pr = 10$, as discussed in the previous section, and for a wide range of Rayleigh and Reynolds numbers: $Ra \leq 8000$ and $Re \leq 2$. At this point, the Reynolds number Re is increased from zero to uncover the effect of throughflow. The onset of convective instability is determined first using a temporal stability analysis, since critical spatial growth rates are zero at this onset. In other words, perturbations can be decomposed into normal modes with complex frequencies and real wave numbers.

Longitudinal rolls ($k_x = 0$, $k = k_y$), which are helicoidal rolls with their axes parallel to the throughflow direction, are not affected by the throughflow. Their instability characteristics are the same as those obtained without throughflow

($Re = 0$). Hence, they appear as stationary rolls in the weakly elastic regime and oscillatory rolls in the strongly elastic regime. Since these results are already known, the remaining section focuses on linear properties of TRs ($k_x = k$, $k_y = 0$), whose axes are perpendicular to the throughflow direction. The characteristics of three-dimensional oblique rolls can be easily deduced from TRs using the inverse Squire transformation.

We first consider the transition from stable to convectively unstable regimes of weakly elastic fluids. Having used the approximate dispersion relation to provide initial estimates about the throughflow influence, converged results are generated by applying the shooting method to the full dispersion relation and analyzed in detail next. Fig. 2 shows critical stability curves for the Rayleigh number, wave number and oscillation frequency as functions of the Reynolds number for $\lambda_1 = 0.025$ and different values of Γ. It can be observed from these figures that, in the absence of throughflow ($Re = 0$), the weak elasticity of the fluid does not influence the onset of convective instability and the critical values Ra_c, k_c, and ω_c are the same as those of a Newtonian fluid ($\Gamma = 1$). As expected in this case, a pitchfork bifurcation is observed for all Γ, even in the limiting case of a Maxwell fluid ($\Gamma = 0$), also presented for comparison purposes.

At any given finite but non vanishing throughflow ($Re \neq 0$), it is clear from Fig. 2(a) that an increase in Γ leads to flow destabilization, i.e. to a reduction in the respective critical Rayleigh number. The least unstable condition corresponds to a Maxwell fluid ($\Gamma = 0$) whereas the most unstable one corresponds to a Newtonian fluid ($\Gamma = 1$). It is important to note that an opposite trend has been observed in a porous medium by Hirata and Ouarzazi (2010). Such a qualitative difference in behavior with respect to the viscosity ratio is likely due to the linear character of Darcy's law, used to model the momentum equations in the porous medium.

Fig. 2(a) also shows the stabilizing effect of throughflow for any fixed value of the viscosity ratio. The critical Rayleigh number at the onset of convective instability Ra_c for the Newtonian fluid case ($\Gamma = 1$) only shows a weak dependence on Re. However, as the viscosity ratio Γ decreases, the throughflow stabilization increases. In other words, Ra_c is an increasing function of Re. Furthermore, the smaller the value of Γ, the more pronounced is this effect. Fig. 2(b) on the other hand, shows a decrease in critical wave number k_c with increasing Re as well as decreasing Γ, both in the weakly elastic regime. This implies that emerging transversal convection rolls have a larger cross-section when the throughflow is moderate and/or the polymer concentration is high. The dependence of the critical oscillatory frequency ω_c on Re is shown in Fig. 2(c). Its value decreases with a decreasing Γ, although this effect is nearly negligible at small Re. The dimensionless critical phase velocity V_φ^*/U_0^*, averaged over the range of Reynolds numbers shown in this figure, varies from 0.83 for Maxwellian fluids ($\Gamma = 0$) to 0.86 for Newtonian fluids ($\Gamma = 1$). Hence, the addition of polymer molecules to a solution with very weak elasticity has no significant effect on the phase velocity of TRs.

Finally, it is worth noting that the insets in Fig. 2 show comparisons between the converged numerical results obtained from the full dispersion relation using a shooting method with the approximate analytical results obtained from the algebraic dispersion relation generated using a single-term Galerkin expansion. A fairly good agreement is observed for low values of the Reynolds number. When the Reynolds number exceeds $Re = 0.3$, the approximate results start to significantly diverge from the converged numerical ones.

The onset of convective instability is now addressed for strongly elastic solutions. Three bifurcating convective solutions exist. The three unstable modes for $Re > 0$ are : (i) the stationary unstable mode (S) in the $Re = 0$ limit, i.e. $\omega_c(Re \to 0) = 0$; (ii) the mode for which $\omega_c(Re \to 0) > 0$, characterizing downstream traveling waves (TWD); and (iii) the mode for which $\omega_c(Re \to 0) < 0$, characterizing upstream traveling waves (TWU).

In order to evaluate effect of elasticity alone, $\lambda_1 = 0.1$ and $\lambda_1 = 0.3$ cases are investigated with a fixed $\Gamma = 0.15$. On the other hand, the effect of viscosity ratio alone is studied by fixing $\lambda_1 = 0.3$ and investigating the $\Gamma = 0.15$ and $\Gamma = 0.75$ cases. Four different cases are shown in Fig. 3, which represent the true critical Rayleigh number, wave number, oscillatory frequency and phase speed at the onset of convective instability. It includes all possible parameter combinations between $\lambda_1 = 0.1$ and 0.3 and $\Gamma = 0.15$ and 0.75. It is important to note that the case with $\lambda_1 = 0.1$ and $\Gamma = 0.75$ represents a weakly elastic solution and was included as a solid line without symbols for comparison purposes. As expected for strongly elastic solutions, a Hopf bifurcation occurs for all three combinations of rheological parameters in the limit of zero Reynolds number. In this limit, the critical Rayleigh numbers which mark the onset of oscillatory convective instability are $Ra_c^o = 950.05$ for $\lambda_1 = 0.1$ and $\Gamma = 0.15$ as well as $Ra_c^o = 484.57$ for $\lambda_1 = 0.3$ and $\Gamma = 0.15$, besides $Ra_c^o = 1574.77$ for $\lambda_1 = 0.3$ and $\Gamma = 0.75$. This indicates that Ra_c^o decreases with an increasing λ_1 and increases with an increasing Γ when $Re = 0$. Such a respectively destabilizing / stabilizing role of these rheological parameters is maintained at nonzero but still low Reynolds numbers, but is reversed beyond a high enough Reynolds number.

5. TRANSITION TO ABSOLUTE INSTABILITY

Having determined the onset of convective instability for this flow field, it is now possible to verify when a transition to absolute instability occurs, if it occurs at all. In the present paper, this transition is studied for TRs only. As done in section 4. weakly elastic solutions are considered first, followed by their strongly elastic counterparts. Furthermore, $Pr = 10$ for all cases examined here.

The first set of results presented in this section involve fluids with a weak elasticity of $\lambda_1 = 0.025$. Viscosity ratio influence is quantified by considering two values of Γ, namely $\Gamma = 0.15$ and $\Gamma = 0.75$, which correspond to concentrated

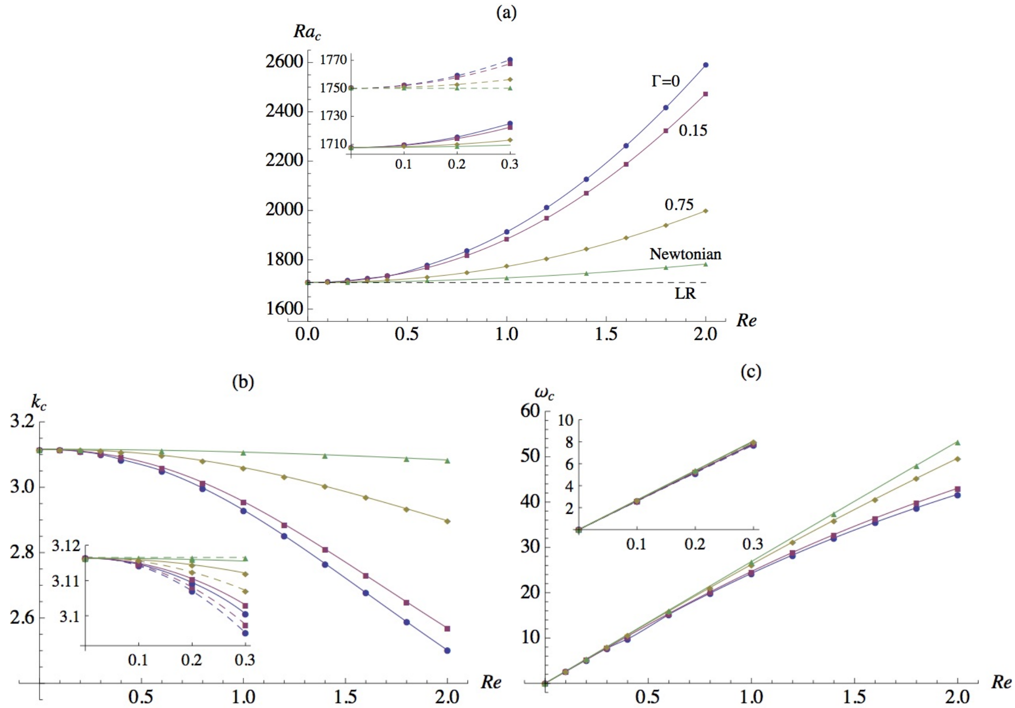

Figure 2. Critical (a) Rayleigh number, (b) wave number, and (c) oscillation frequency at the onset of convective instability for weakly elastic TRs with $\lambda_1 = 0.025$ and different values of Γ, including the Newtonian fluid case ($\Gamma = 1$). The threshold of LRs (dashed line) is also presented. TR comparisons between full dispersion relation (solid lines) and approximate dispersion relation (dashed lines) are shown in the insets.

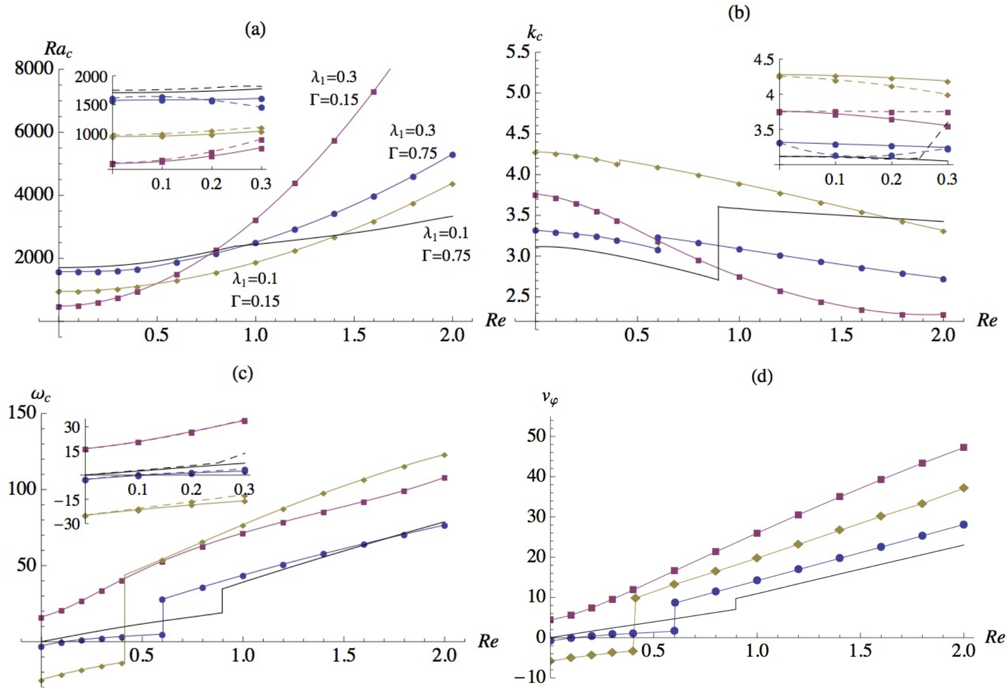

Figure 3. Critical (a) Rayleigh number, (b) wave number and (c) oscillation frequency, (d) phase speed at the onset of convective instability for strongly elastic TRs with $\lambda_1 = 0.3$ and $\Gamma = 0.75$ ($Re_{c2} = 0.603077$), $\lambda_1 = 0.3$ and $\Gamma = 0.15$ as well as $\lambda_1 = 0.1$ and $\Gamma = 0.15$ ($Re_{c2} = 0.41291$). Weakly elastic TRs with $\lambda_1 = 0.1$ and $\Gamma = 0.75$ (solid lines without symbols) also presented.

and diluted solutions, respectively. Fig. 4 displays the onset of convective and absolute instability for these two cases, as well as a Newtonian fluid case for comparison purposes, as functions of the Reynolds number. Ra_c corresponds to the Rayleigh number of the first threshold, beyond which the base state favors the emergence of convectively unstable stationary TRs when $Re = 0$ and downstream moving TRs when $Re > 0$. These bifurcation thresholds have already

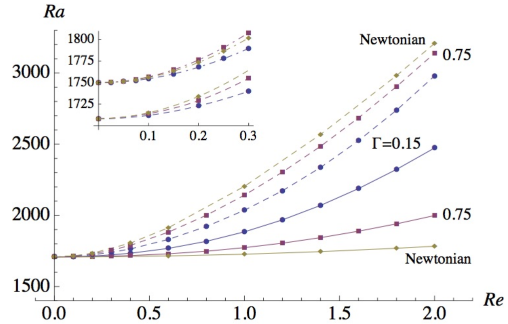

Figure 4. Thresholds for the onsets of convective (solid lines) and absolute (dashed lines) instabilities for weakly elastic solutions with $\lambda_1 = 0.025$ and two different values of Γ. Newtonian case is included for comparison purposes. A comparison between the full dispersion relation (dashed lines) and approximate dispersion relation (dot-dashed lines) are shown in the insets.

been determined through a temporal stability analysis in the previous section. Ra_A corresponds to the Rayleigh number of the second threshold, beyond which the convectively unstable disturbances become absolutely unstable. It has been obtained from a saddle point analysis of the differential dispersion equation solution, which is numerically obtained with the shooting method. In other words, one can say that the base state is stable when $Ra < Ra_c$, convectively unstable when $Ra_c < Ra < Ra_A$ and absolutely unstable $Ra > Ra_A$, assuming TRs are the first to become absolutely unstable. The onset of instability is absolute for $Re = 0$, i.e. $Ra_c = Ra_A$. However, a region of convective instability is created in the presence of throughflow and this region increases with an increasing Re. Furthermore, the absolute instability threshold Ra_A increases with an increasing Γ, whereas an opposite trend was observed for the convective instability threshold Ra_c. Such a behavior reduces (extends) the convectively unstable region for concentrated (diluted) viscoelastic solutions. As a consequence, the boundary between convective and absolute instability for weakly elastic fluids remains below the one corresponding to Newtonian fluids.

Temporal stability analysis performed in section 4revealed that in strongly elastic solutions, the basic state becomes unstable against three different types of extended perturbations: S, TWU and TWD at the bifurcation threshold Ra_c^S, Ra_c^U and Ra_c^D respectively. The borderlines between convective and absolute instability of the three modes of instability are determined first for a representative case with $\lambda_1 = 0.3$ and $\Gamma = 0.15$. It is found that the absolute instability threshold corresponding to S mode rapidly increases with Re and diverges even for a small through-flow. The threshold of absolute instability for S mode is much higher than the one corresponding to both TWU and TWD for all Reynolds numbers considered here.

The onset of absolute instability is now determined for the same four viscoelastic parameter combinations discussed in Fig. 3. In the presence of throughflow, the onset of absolute instability always occurs for TWU first, regardless of viscoelastic parameters selected in the strongly elastic regime. Therefore, only the characteristics of TWU are discussed in the remaining of this section. Figures 5(a) and 5(b) present the Rayleigh numbers and spatial growth rates, respectively, at the onset of absolute instability as functions of the Reynolds number with their onset of convective instability included for comparison purposes. This figure shows the existence of a finite region of convective instability for $Re = 0$ as it was found in the $\lambda_1 = 0.3$ and $\Gamma = 0.15$ case. This figure also shows that the thresholds of convective Ra_c and absolute Ra_A instability coincide at $Re = Re^* = 0.188785$ (see inset of Fig. 5(a) which corresponds to the $\lambda_1 = 0.3$ and $\Gamma = 0.75$ case). Hence, at this Reynolds number, the basic state becomes absolutely unstable without passing through a convective instability region, in opposition to what is observed for all other values of Re. Although not entirely clear in the inset of Fig. 5(a), this can be observed in 5(b), since the spatial growth rate at the onset of absolute instability must be zero under these circumstances. This may be physically interpreted as the point where the group velocity vanishes at the onset of convection (i.e. $Ra = Ra_c$). The convectively unstable region decreases when the Reynolds number is increased up to Re^* and increases when this number is increased beyond Re^*.

6. CONCLUSIONS

In the present paper we investigate the linear stability of viscoelastic fluids subject to a horizontal throughflow and a vertical temperature gradient simultaneously. In the framework of the upper convected Oldroyd-B model, we find that the base state is composed of a non vanishing normal stress component in addition to the shear stress component induced by the Poiseuille flow. The linear and normal perturbation equations are obtained with the software *Mathematica* and solved analytically, using a one-mode Galerkin expansion, as well as numerically, using a shooting method. The influence of the throughflow on the convective and absolute instability thresholds has been analyzed for a wide range of the rheological parameters.

Future work includes a full three-dimensional linear stability analysis for the onset of absolute instability of oblique

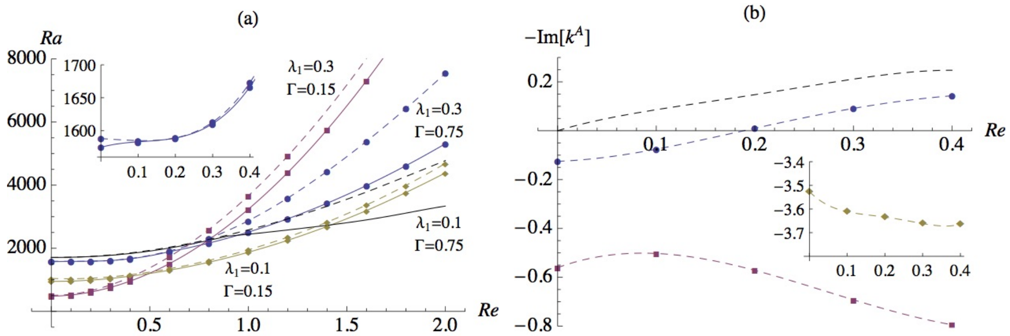

Figure 5. (a) Thresholds for the onsets of convective (solid lines) and absolute (dashed lines) instabilities and (b) spatial growth rates at the onset of absolute instability as functions of the Reynolds number for the same weakly and strongly elastic cases shown in Fig. 3. Both insets present zoomed in data for one or more specific curves.

and longitudinal rolls. It will be pursued by extending the current Galerkin expansion solution procedure, which allows the use of the zero group velocity conditions to facilitate the search for three-dimensional pinching points.

7. REFERENCES

Bird, R.B., Armstrong, R.C. and Hassager, O., 1987. Dynamics of Polymeric Liquids. John Wiley & Sons.

Hirata, S.C., de B. Alves, L.S., Delenda, N. and Ouarzazi, M.N., 2015. "Convective and absolute instabilities in rayleigh-bénard-poiseuille mixed convection for viscoelastic fluids". Journal of Fluid Mechanics, Vol. 765, pp. 167–210. ISSN 1469-7645.

Hirata, S.C. and Ouarzazi, M.N., 2010. "Three-dimensional absolute and convective instabilities in mixed convection of a viscoelastic fluid through a porous medium". Physics Letters, Section A: General, Atomic and Solid State Physics, Vol. 374, No. 26, pp. 2661–2666.

Huerre, P. and Monkewitz, P.A., 1985. "Absolute and convective instabilities in free shear layers." Journal of Fluid Mechanics, Vol. 159, pp. 151–168.

Huerre, P. and Monkewitz, P.A., 1990. "Local and global instabilities in spatially developing flows". Annual Review of Fluid Mechanics, Vol. 22, No. 1, pp. 473–537.

Kolodner, P., 1998. "Oscillatory convection in viscoelastic DNA suspensions". Journal of Non-Newtonian Fluid Mechanics, Vol. 75, No. 2-3, pp. 167–192.

Li, Z. and Khayat, R.E., 2005. "Finite-amplitude Rayleigh-Bénard convection and pattern selection for viscoelastic fluids". Journal of Fluid Mechanics, Vol. 529, pp. 221–251.

Nicolas, X., 2002. "Bibliographical review on the Poiseuille-Rayleigh-Bénard flows: The mixed convection flows in horizontal rectangular ducts heated from below". International Journal of Thermal Sciences, Vol. 41, No. 10, pp. 961–1016.

8. RESPONSIBILITY NOTICE

The authors are the only responsible for the printed material included in this paper.